

# CHITOSAN/ZnO NANOCOMPOSITE MEMBRANES FOR REMOVAL OF PARACETAMOL FROM WATER

LAMINE AOUDJIT\*, EL AMINE NEBBAT\*\* and DJAMILA ZIOUI\*

\*Unité de Développement des Equipements Solaires, UDES/Centre de Développement des Energies Renouvelables, CDER, Bou Ismail, 42415, Tipaza, Algeria

\*\*Faculty of Sciences, Laboratory LSDME, University of Algiers I, Algiers, Algeria

✉ Corresponding author: D. Zioui, ziouidjamila@yahoo.fr

Received February 4, 2023

In this study, chitosan (CS) and zinc oxide (ZnO) nanoparticles were used as photocatalysts for the removal of paracetamol from water. Membranes made of chitosan and zinc oxide were prepared through a simple casting method with various concentrations of ZnO. The characterization was carried out by X-ray diffraction (XRD), Fourier infrared (FTIR) spectroscopy, scanning electron microscopy (SEM), and diffuse reflectance ultraviolet spectroscopy. The chitosan/ZnO composite was investigated for the removal of paracetamol, as a pollutant model, using the photodegradation activity. The effects of parameters such as pH (3–9), composite amount (0.03, 0.06, and 0.09 g), paracetamol concentration (20, 30, 40 ppm), and contact time (30, 60, 90, 120, 150, and 180 min) were studied. The results indicated that the highest photocatalytic degradation was obtained at 3 h of contact time, an initial concentration of 20 ppm, and a solution free pH (6.7). Using these conditions, over 99.17% of paracetamol was able to be degraded using 0.09 g of chitosan-ZnO nanocomposite under solar light irradiation. The obtained composite membranes (chitosan/ZnO) can be used as an effective and economical photocatalyst for complex water purification processes.

**Keywords:** chitosan, chitosan/ZnO, photodegradation, paracetamol

## INTRODUCTION

Nowadays, the world is facing an alarming global concern, which is water contamination. This has a direct impact on human health and ecosystem biodiversity. Pharmaceuticals are among the most critical contaminants of emerging concern for water, because of their extensive use and uncontrolled release. Their presence in aqueous effluents is picked at concentrations from ng/L to mg/L, representing a detrimental impact on aquatic ecosystems and humans.<sup>1,2</sup> One of the most commonly encountered pharmaceutical drugs is paracetamol, also known as acetaminophen (ACT), which is extensively used as an analgesic and antipyretic agent, it is one of the most often prescribed medications around the world.<sup>3</sup> The presence of paracetamol and other drugs in the water poses a threat to human health and the environment, because of its toxicity, bioaccumulation in living organisms, and resistance to biological degradation processes. The extensive presence of paracetamol and other persistent contaminants in water bodies is caused by its ineffective removal from effluents by a

number of methods employed by scientists for the removal of diverse pollutants, such as biological treatment, filtration, ozonation, gravity separation, flotation-coagulation, membrane processes, reverse osmosis, disinfection by ultraviolet (UV) radiation, solar wastewater treatment, distillation, adsorption, and advanced oxidation processes.<sup>4-13</sup> From all these methods, advanced oxidation processes and, in particular, photocatalysis have attracted great interest as they offer significant advantages when it comes to costs, easy usability, and the effective use of solar energy for the degradation of organic pollutants.<sup>14-17</sup>

Zinc oxide (ZnO) is one of the most promising semiconductors, with a wide band gap of 3.37 eV, and remarkable physical and chemical properties, including high electron mobility, good transparency, strong luminescence, UV-blocking ability, environmental friendliness, biodegradation, and photocatalytic activity.<sup>18-19</sup> However, its application in photocatalytic degradation is limited because of the difficulty in separating the photocatalyst and it is normally a

less active photocatalyst. In order to address the problem and overcome this limitation, its immobilization into polymeric substrates, whose porosity and pore size can be controlled, is an attractive alternative.

Chitosan biopolymer is obtained via N-deacetylation of chitin, which is the second most abundant natural polysaccharide after cellulose.<sup>20-21</sup> It has attracted special attention due to its biocompatibility, biodegradability, bio-renewability, non-toxicity and cost-effectiveness, compared to other materials used in water treatment applications. The modification of chitosan (CS) with nanomaterials, specifically metal oxide nanoparticles, has gained great attention as a result of the high value added to their properties.<sup>20-21</sup>

In the present study, our aim was to develop new chitosan/ZnO photocatalyst composite membranes prepared via the casting method for the removal of paracetamol as a model pollutant under solar light irradiation.

## EXPERIMENTAL

### Materials and methods

Paracetamol ( $M = 151.16$  g/mol), with the chemical formula  $C_8H_9NO_2$ , 99% purity, and a maximum absorption at a wavelength of 243 nm, was purchased from Merck. Chitosan was supplied by Pelican Biotech and Chemicals Labs, Kerala (India). Zinc oxide was purchased from Sigma-Aldrich Co. Acetic acid (purity 99.9%), and sodium hydroxide (98%, purity) were purchased from Biochem Chemopharma. All solutions were prepared with ultrapure Milli-Q water.

The characterization of the samples was performed based on the crystal structure of the chitosan-ZnO, which was evaluated by X-ray diffraction (XRD) using a Bruker D8 Discover diffractometer with incident CuK (40 kV and 30 mA). The Fourier-transform infrared spectroscopy (FTIR) spectra of chitosan-ZnO as prepared were recorded in a JASCO 460 Plus model FTIR Spectrometer in the region of  $400\text{--}4000$   $\text{cm}^{-1}$ , and the sample was prepared as KBr pellets under high pressure. Scanning electron microscopy (SEM) was carried out with a Quanta 650 SEM to access the morphology and microstructure of the membrane. Solubility in water was defined as the percentage of the dry matter of a film that is solubilized after 24 hours of immersion in water.

The density was measured by weighing the same area of samples in the dry state, expressed as the mass ratio (mg)/area ( $\text{cm}^2$ ), and the thickness of the membranes was calculated using a digital micrometer. Water contact angle measurements were performed by the sessile drop method.<sup>5,21</sup> Light transmittance and opacity were measured at a wavelength of 600 nm using an ultraviolet (UV) spectrophotometer

(Shimadzu UV1800), according to the methodology described by Zioui *et al.*<sup>21</sup> High-performance liquid chromatography (Agilent HPLC 1100) was employed to assess paracetamol mineralization.

The photocatalytic degradation of paracetamol was carried out in a glass Petri dish with a 250 mL capacity volume. For the photocatalytic assays, 150 mL of paracetamol standard solution with the chitosan/ZnO membrane (0.09 g) was kept in the dark for 30 min. After that, the glass Petri dish was placed under magnetic agitation and sunlight irradiation for 3 h, and 3 mL aliquots were withdrawn hourly. All the withdrawn samples were analyzed with a UV-visible spectrophotometer (Shimadzu-1800) and the peak at 243 nm was used to monitor paracetamol absorbance over irradiation time. The percentage of degradation was estimated using the following equation:<sup>1,13,20</sup>

$$\text{Degradation (\%)} = \frac{C_0 - C_t}{C_0} \times 100 \quad (1)$$

where  $C_0$  is the initial dye concentration and  $C_t$  is the paracetamol concentration after a certain reaction time  $t$  (min).

### Preparation of composite films

The chitosan-ZnO nanocomposite membranes were prepared using the casting technique. First, chitosan (0.4 g) was dissolved in 20 mL of 2% acetic acid solution, which was then stirred at 30 °C until the chitosan had completely dissolved, as described in our previous work.<sup>20,21</sup> After stirring, different amounts of nano-ZnO (0.03, 0.06, and 0.09 g) were added, the mixture was magnetically stirred at room temperature for 3 hours to obtain a homogenous solution. The formed solutions were cast into Petri dishes and dried in an electric oven at 60 °C for 6 hours. The obtained membranes were treated with sodium hydroxide solution and washed with distilled water. The characterization and photocatalytic activity of the prepared films were further evaluated.

## RESULTS AND DISCUSSION

Figure 1 shows the X-ray diffraction patterns of the pure CS membrane and CS/ZnO composite membranes. The peaks at  $2\theta < 25^\circ$  are characteristic of chitosan (slightly amorphous) (Fig. 1). Similar observations were reported in previous studies.<sup>20,21</sup> In the XRD pattern of the CS/ZnO composite membranes (Fig. 1), other diffraction peaks (at  $2\theta = 31.7^\circ, 34.4^\circ, 36.2^\circ, 47.5^\circ, 56.6^\circ, 62.8^\circ, 66.3^\circ, 67.9^\circ, \text{ and } 69.1^\circ$ ) were assigned to (100), (002), (101), (102), (110), (103), (200), (112), (201) and (004) crystal planes of hexagonal zinc oxide. These peaks are consistent with the database of the Joint Committee on Powder Diffraction Standards (JCPDS file, PDF No. 36-1451). These data revealed the successful formation of ZnO in the

composite membranes by the casting technique. The introduction of ZnO in chitosan decreased the crystallinity of the composite membranes and increased the flexibility of the polymer chain.<sup>22</sup>

The infrared spectrum for chitosan and chitosan/ZnO is shown in Figure 2. A strong band in the region of  $3459\text{ cm}^{-1}$  corresponds to N–H and O–H stretching. The absorption peaks at  $1678$ ,  $1438$ ,  $1373\text{ cm}^{-1}$  were associated with the presence of the C=O stretching of the amide I band, bending vibrations of the N–H and C–H bending, respectively. The adsorption peaks at  $1574$ ,  $1373$ , and  $1024\text{ cm}^{-1}$  are assigned to amide. The peaks in the low-frequency region at  $573$

$\text{cm}^{-1}$  was attributed to the ZnO bonds, suggesting the cross-linking of zinc to chitosan. These results are in harmony with those reported in similar works.<sup>23-25</sup>

In comparison with CS, the increase in the intensity of CS/ZnO in the band range of  $3277$  to  $3459\text{ cm}^{-1}$  with the incorporation of ZnO suggests the formation of new interactions between ZnO molecules and the binding sites of chitosan ( $\text{NH}_2$  and OH groups of CS). It can be observed in the FTIR spectra of CS and chitosan/ZnO the presence of the characteristic peaks, which are related to the chitosan and ZnO.

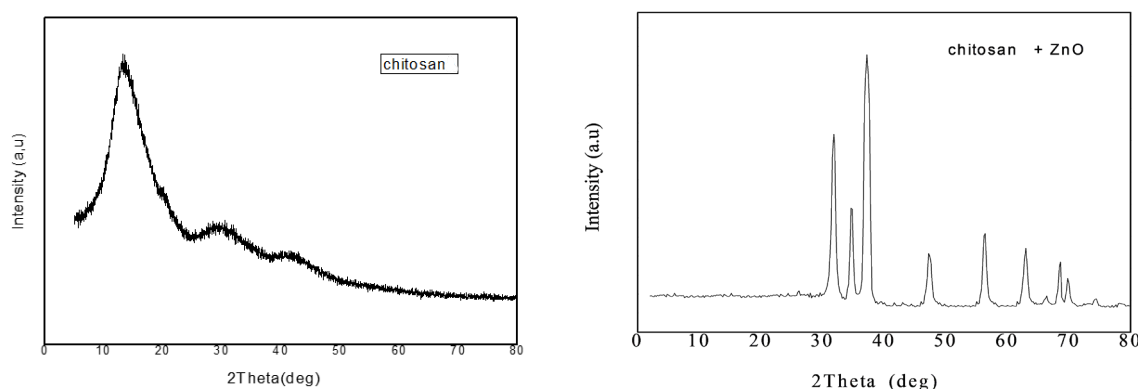


Figure 1: XRD patterns of chitosan and chitosan/ZnO composite membrane

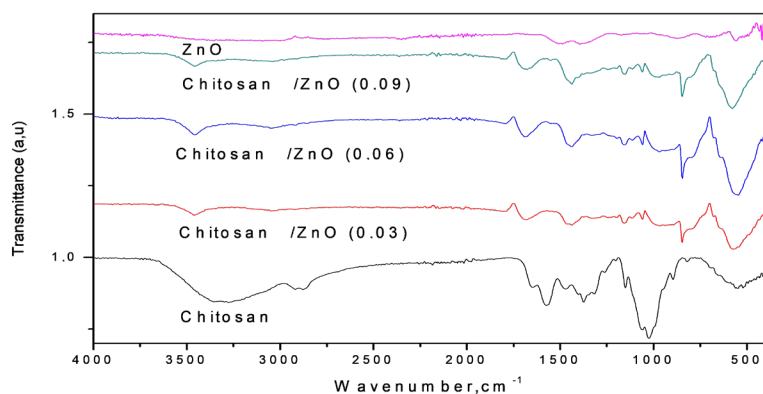


Figure 2: FTIR spectra of chitosan, chitosan/ZnO composite membranes and ZnO nanoparticles

SEM images of chitosan and chitosan/ZnO revealed that the morphologies and texture have changed upon the introduction of the ZnO nanoparticles. Homogeneous dispersion of ZnO nanoparticles over the surface of chitosan is one of the most important factors to increase the photocatalytic activity of the nanocomposites.

The data tabulated in Table 1 indicate an increase in thickness with the incorporation of ZnO. Transmittance measurements of the composite films were slightly reduced at 77%,

76.3% and 73% with the incorporation of ZnO (0.03, 0.06 and 0.09 g), compared to that of the pure chitosan film, which was 97.4%, as shown in Figure 4. The explanation of the changes in transmittance can be high UV absorption and scattering by ZnO.

The nanocomposite exhibited slightly increased water contact angle and lower water content, but with no statistical significance.<sup>25,26</sup> This could be explained by the fact that the higher nanoparticle concentration in the film led to the

formation of more hydrogen bonds between ZnO and the polymer matrix, resulting in less

interaction between water molecules and nanocomposite films.

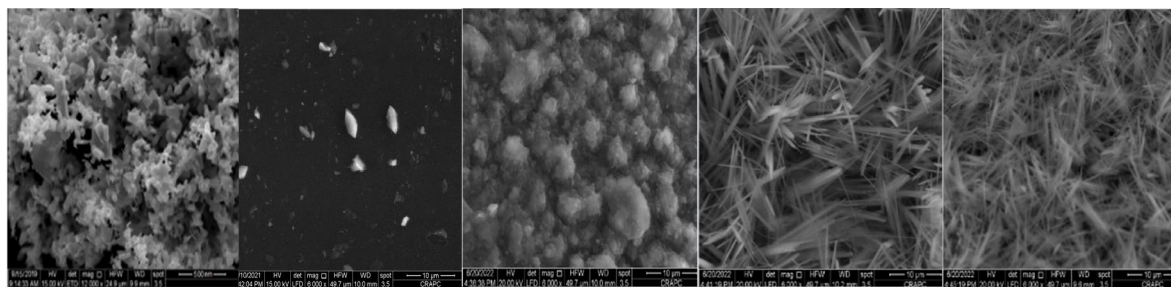


Figure 3: SEM images of ZnO nanoparticles, chitosan film and chitosan composite film with different amounts of nano-ZnO (0.03, 0.06 and 0.09 g)

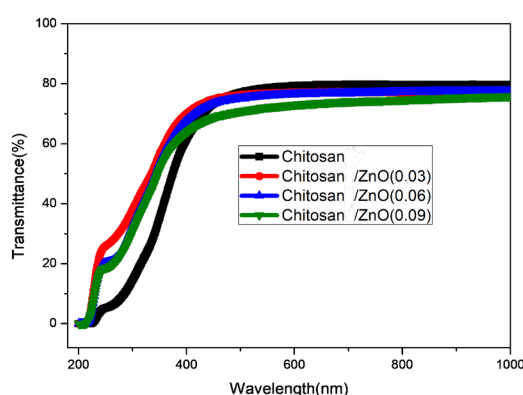


Figure 4: Transmittance of chitosan film and chitosan composite film with different nano-ZnO amounts (%)

Table 1  
Chemical and physical characteristics of synthesized membranes

Membranes	Thickness (μm)	Density (mg/cm <sup>2</sup> )	Water content (%)	Contact angle (deg)
Chitosan	50	0.009	33	69
Chitosan/ZnO (0.03)	150	0.011	32.75	77
Chitosan/ZnO (0.06)	200	0.017	30.15	78
Chitosan/ZnO (0.09)	300	0.020	8.95	80

### Photocatalytic activity of the chitosan/ZnO composite film

The photocatalytic activity of the chitosan-ZnO nanocomposite membrane comprising 0.09 g of ZnO nanoparticles was used in this work to assess the degradation of paracetamol. Figure 5 shows the degradation profile of paracetamol (20 mg/L) after 3 h of sunlight irradiation, indicating that approximately 99.17% of the paracetamol was degraded. Two initial experiments were conducted as a control to understand the role of adsorption and photolysis on the paracetamol degradation process under the same conditions (Fig. 5). For the adsorption assay, the solution

was placed in contact with the chitosan-ZnO nanocomposite membranes without any light source. The paracetamol solution was placed under solar radiation for the photolysis assay, without the chitosan-ZnO nanocomposite membranes. After 3 h of experiment, an adsorption of 23% of paracetamol was observed, indicating that the chitosan-ZnO nanocomposite membranes have a slight affinity for paracetamol. The photolysis experiment showed low degradation (6%) after 3 h, confirming the high stability and resilience of paracetamol and the need for photocatalytic processes.<sup>2</sup>

### Effect of initial paracetamol concentration

In order to study the influence of the initial concentration of pollutant ( $C_0$ ) on the efficiency of photocatalysis for the degradation of paracetamol (PAR), we varied its concentration over a range from 20 to 40 mg/L at free pH (6.7) and a dose of 0.09 g of nanoparticles. The curve illustrated in Figure 6 represents the evolution of the degradation rate of paracetamol for different initial concentrations of the pollutant for 180 min. The results obtained indicate that the degradation of paracetamol is more remarkable when the initial concentration is lower. The degradation rate for a low concentration of substrate (20 mg/L) gives a high yield, – about 99.17%, for a solar irradiation time of 180 min, whereas for an initial concentration of 30 and 40 mg/L the degradation decreases to 94%. In other words, the efficiency of degradation decreases when the pollutant concentrations increase. Our results are in agreement with those found in other works.<sup>2,15,17,19</sup> The presumed reason is that for high pollutant concentrations, the generation of radicals ( $\text{OH}^\cdot$ ) on the surface of the photocatalyst

is reduced since the active sites are covered by the pollutant molecules. This slows down the generation of the active species responsible for the photocatalytic reaction. In addition, a concentrated solution forms a screen, which weakens the penetration of light, unlike low concentrations. The degradation of the pollutant is therefore inversely proportional to its initial concentration.

### Effect of pH value on paracetamol degradation

To assess the influence of pH, we observed the photocatalytic degradation of paracetamol at different pH values. In order to study the influence of pH on the kinetics of paracetamol degradation, a series of experiments was carried out using the same experimental conditions as the previous one ( $C_0 = 20$  mg/L,  $[\text{ZnO}/\text{chitosan}] = 0.09$  g,  $V = 150$  mL), but this time by initially fixing the pH of the solution by adding sodium hydroxide (NaOH) for basic media and hydrochloric acid (HCl) for acidic media. The results obtained are illustrated in Figure 7.

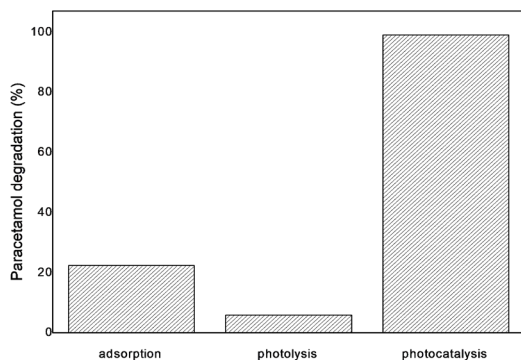


Figure 5: Photocatalytic degradation of PAR (20 mg/L) with 0.09 g ZnO/chitosan film after over 3 h of sunlight irradiation; controls: irradiation of PAR solution without the film (photolysis), and the film in PAR solution with no irradiation (adsorption)

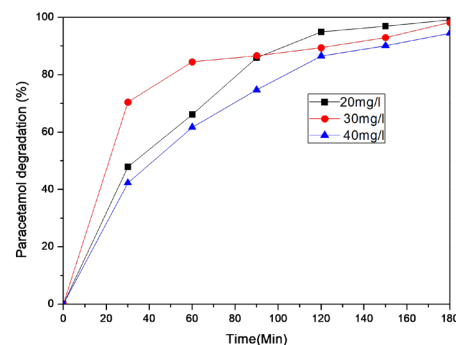


Figure 6: Effect of initial paracetamol concentration (at free pH (6.7) and using chitosan/ZnO (0.09g)) on the degradation efficiency of paracetamol

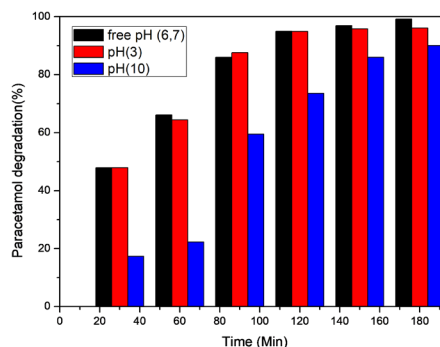


Figure 7: Effect of pH on paracetamol degradation ( $[\text{PAR}] = 20$  mg/L, using chitosan/ZnO (0.09 g))

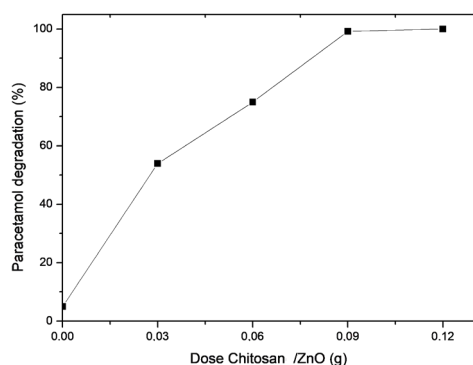


Figure 8: Effect of ZnO catalyst dose on the photocatalytic degradation ([PAR] = 20 mg/L and free pH (6.7))

These results clearly show the influence of the pH of the medium on the degradation of paracetamol and that the greatest efficiency of the degradation was obtained for a free pH (6.7) with 99.17% degradation during 180 min. These results are in harmony with those obtained by Aoudjit *et al.*<sup>20</sup> Moreover, we found that, whatever the pH of the solution was, the paracetamol still degraded, nevertheless with a degradation rate of 90% for the basic pH (10) and 96% at the acid pH (3). The free pH is chosen as an optimal pH value for our study.

#### Effect of pH value on paracetamol degradation

To assess the influence of pH, we observed the photocatalytic degradation of paracetamol at different pH values. In order to study the influence of pH on the kinetics of paracetamol degradation, a series of experiments was carried out using the same experimental conditions as the previous one ( $C_0 = 20$  mg/L, [ZnO/chitosan] = 0.09 g,  $V = 150$  mL), but this time by initially fixing the pH of the solution by adding sodium hydroxide (NaOH) for basic media and hydrochloric acid (HCl) for acidic media. The results obtained are illustrated in Figure 7. These results clearly show the influence of the pH of the medium on the degradation of paracetamol and that the greatest efficiency of the degradation was obtained for a free pH (6.7) with 99.17% degradation during 180 min. These results are in harmony with those obtained by Aoudjit *et al.*<sup>20</sup> Moreover, we found that, whatever the pH of the solution was, the paracetamol still degraded, nevertheless with a degradation rate of 90% for the basic pH (10) and 96% at the acid pH (3). The

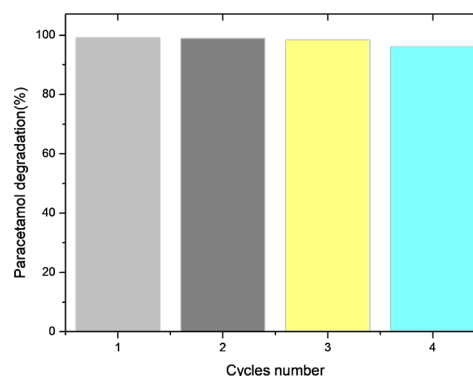


Figure 9: Photodegradation of paracetamol over 4 catalytic cycles in sunlight ([PAR] = 20 mg/L, free pH = 6.7, using chitosan/ZnO (0.09 g))

free pH is chosen as an optimal pH value for our study.

#### Effect of catalyst dose of ZnO

In order to better understand the influence of catalyst dose on the photocatalysis of paracetamol, different amounts of ZnO catalyst (0.03, 0.06, 0.09 and 0.12 g) were tested for the photocatalytic degradation studied. The curve shown in Figure 8 represents the rate of degradation of paracetamol in the presence of ZnO/chitosan containing different quantities of ZnO after 180 min of reaction. From the results obtained, it was observed that the rate of degradation increases as the quantity of the catalyst increases. For a dose of ZnO/chitosan = 0.09 g, the yield reached more than 99% after 180 min. Thus, the yield of the photodegradation is proportional to the quantity of the catalyst. The improvement in the degradation rate is due to the increase in active sites for the production of OH<sup>-</sup> free radicals.

#### Reusability of the chitosan-ZnO nanocomposite membranes

An efficiency test by recycling was done. After each treatment for 180 min, the same catalyst already used was washed with distilled water and dried in an oven. The results of the study of the photodegradation efficiency of paracetamol, under solar radiation, after reuse of recycled catalysts (Fig. 9) show that zinc oxide/chitosan maintains the same photocatalytic performance after three consecutive cycles, with a constant yield (98%) for a solar irradiation duration of 180 min. These results are in harmony with those reported in similar works.<sup>20,21</sup> It can be

concluded that the chitosan/ZnO membrane is a promising material for environmental remediation.

### Mineralisation and degradation of paracetamol

HPLC was used to analyze the treated solution after 180 min of treatment at free pH (6.7), as presented in Figure 10. The main peak is observed at the retention time ( $T_r = 5.43$  min) of paracetamol, which gradually decreases during the degradation period of 180 min. During the

degradation, there appear several peaks that can be ascribed to the intermediates of paracetamol degradation. They are most likely hydroquinone, benzoquinone, p-nitrophenol, and 1, 2, 4-trihydroxybenzene. These intermediates were also determined for paracetamol degradation by means of other advanced oxidation processes.<sup>27</sup> The percentages of degradation and mineralization of paracetamol under solar radiation were 98% and 50.95%, respectively. It can be seen that the mineralization was slower than the degradation due to the formation of intermediate products.

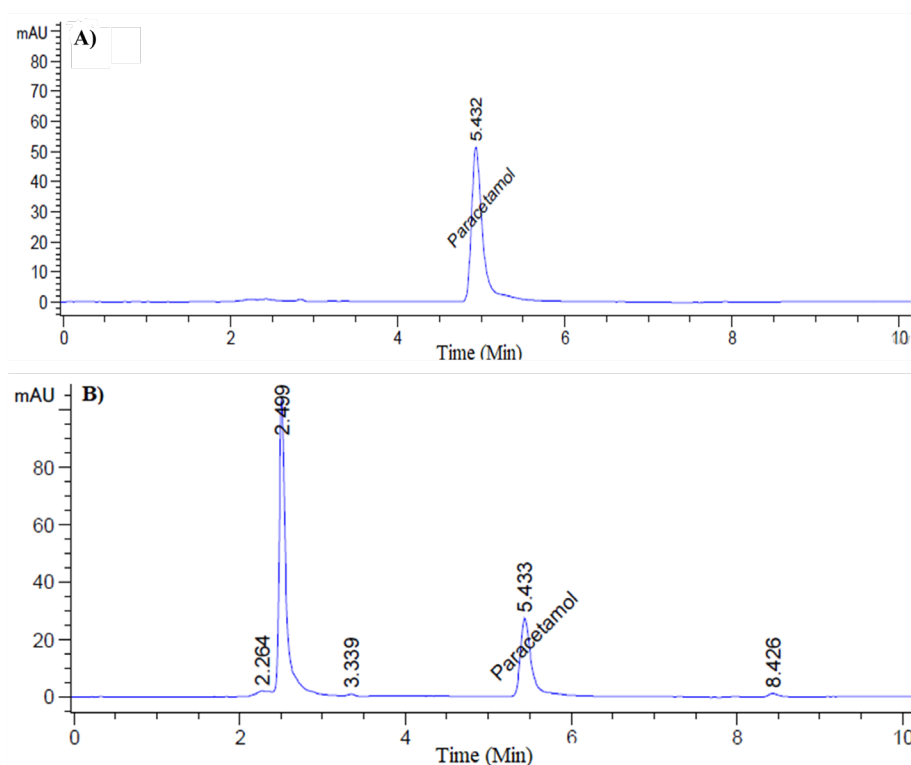


Figure 10: HPLC chromatograms of paracetamol samples (A) before and (B) after 3 h of degradation ([PAR] = 20 mg/L; recirculation time: 3 h; pH free = 6.7)

### CONCLUSION

In this study, chitosan-ZnO nanocomposite membranes were prepared using the casting technique, by immobilizing ZnO nanoparticles in a chitosan (CS) matrix, and were then applied to remove paracetamol from water systems. FTIR analysis confirmed the existence of the relevant functional groups of both chitosan polymer and ZnO in the composite membranes, while the XRD spectra indicated that the chemical structure of ZnO did not change after the immobilization on the chitosan film. SEM images confirmed the incorporation of ZnO molecules into the polymer

matrix of the chitosan surface. The composite film containing 0.09 g of ZnO showed high photocatalytic activity.

In conclusion, the chitosan-ZnO nanocomposite has high photocatalytic capacity and is an eco-friendly strategy for paracetamol removal. Therefore, it could be used in water treatment processes.

**ACKNOWLEDGEMENTS:** This work was supported by the Solar Equipment Development Unit (UDES), Algeria.

## REFERENCES

- <sup>1</sup> L. Aoudjit, H. Salazar, D. Zioui, A. Sebti, P. M. Martins *et al.*, *Polymers*, **13**, 3718 (2021), <https://doi.org/10.3390/polym13213718>
- <sup>2</sup> L. Aoudjit, H. Salazar, D. Zioui, A. Sebti, P. M. Martins *et al.*, *Membranes*, **12**, 849 (2022), <https://doi.org/10.3390/membranes12090849>
- <sup>3</sup> S. Wu, L. Zhang and J. Chen, *Appl. Microbiol. Biotechnol.*, **96**, 875 (2012), <https://doi.org/10.1007/s00253-012-4414-4>
- <sup>4</sup> P. M. Martins, H. Salazar, L. Aoudjit, R. Gonçalves, D. Zioui *et al.*, *Chemosphere*, **262**, 128300 (2021), <https://doi.org/10.1016/j.chemosphere.2020.128300>
- <sup>5</sup> D. Zioui, O. Arous, N. Mameri, H. Kerdjoudj, M. San Sebastian *et al.*, *J. Hazard. Mater.*, **336**, 188 (2017), <https://doi.org/10.1016/j.jhazmat.2017.04.035>
- <sup>6</sup> H. Aburideh, Z. Tigrine, L. Aoudjit, Z. Belgroun, K. Redjimi *et al.*, *Cellulose Chem. Technol.*, **55**, 1153 (2021), <https://doi.org/10.35812/CelluloseChemTechnol.2021.55.99>
- <sup>7</sup> D. Zioui, L. Aoudjit, Z. Tigrine and H. Aburideh, *Cellulose Chem. Technol.*, **56**, 353 (2022), <https://doi.org/10.35812/CelluloseChemTechnol.2022.56.31>
- <sup>8</sup> D. Zioui, L. Aoudjit, Z. Tigrine, H. Aburideh and O. Arous, *Russ. J. Phys. Chem. A*, **96**, 1334 (2022), <https://doi.org/10.1134/S0036024422060334>
- <sup>9</sup> S. Igoud, B. Boutra, L. Aoudjit, A. Sebti, F. Khene *et al.*, in *Procs. 7<sup>th</sup> International Renewable and Sustainable Energy Conference (IRSEC)*, 2019, p. 1, <https://doi.org/10.1109/IRSEC48032.2019.9078228>
- <sup>10</sup> S. Igoud, D. Zeriri, L. Aoudjit, B. Boutra, A. Sebti *et al.*, *Irrig. Drain.*, **70**, 243 (2021), <https://doi.org/10.1002/ird.2540>
- <sup>11</sup> B. Boutra, L. Aoudjit, F. Madjene, H. Lebig, A. Sebti *et al.*, in *ACM International Conference Proceeding Series*, 24-26 September 2015, a13, <http://dx.doi.org/10.1145/2832987.2833008>
- <sup>12</sup> S. Igoud, D. Zeriri, B. Boutra, A. Mameche, Y. Benzegane *et al.*, *Petrol. Sci. Technol.*, **40**, 92 (2022), <https://doi.org/10.1080/10916466.2021.2002358>
- <sup>13</sup> D. Zioui, P. M. Martins, L. Aoudjit, H. Salazar and S. Lanceros-Mendez, *Polymers*, **15**, 1143 (2023), <https://doi.org/10.3390/polym15051143>
- <sup>14</sup> A. Sebti, B. Boutra, M. Trari, L. Aoudjit and S. Igoud, in *Procs. International Conference in Artificial Intelligence in Renewable Energetics*, vol. 102, 2020, p. 143, <https://doi.org/10.1007/978-3-030-37207-1>
- <sup>15</sup> L. Aoudjit, P. M. Martins, F. Madjene, D. Y. Petrovykh and S. Lanceros-Mendez, *J. Hazard. Mater.*, **344**, 408 (2018), <https://doi.org/10.1016/j.jhazmat.2017.10.053>
- <sup>16</sup> D. Zioui, H. Salazar, L. Aoudjit, P. M. Martins and S. Lanceros-Méndez, *Polymers*, **12**, 42 (2020), <https://doi.org/10.3390/polym12010042>
- <sup>17</sup> F. Aoudjit, F. Touahra, L. Aoudjit, O. Cherifi and D. Halliche, *Water Sci. Technol.*, **82**, 2837 (2020), <https://doi.org/10.2166/wst.2020.519>
- <sup>18</sup> T. Bouarroudj, L. Aoudjit, L. Djahida, B. Zaidi, M. Ouraghi *et al.*, *Water Sci. Technol.*, **83**, 2118 (2021), <https://doi.org/10.2166/wst.2021.106>
- <sup>19</sup> F. Ghribi, M. Sehailia, L. Aoudjit, F. Touahra, D. Zioui *et al.*, *J. Photochem. Photobiol. A*, **397**, 112510 (2020), <https://doi.org/10.1016/j.jphotochem.2020.112510>
- <sup>20</sup> L. Aoudjit, D. Zioui, F. Touahra, S. Mahidine and K. Bachari, *Russ. J. Phys. Chem. A*, **95**, 1069 (2021), <https://doi.org/10.1134/S0036024421050034>
- <sup>21</sup> D. Zioui, L. Aoudjit, F. Touahra and K. Bachari, *Cellulose Chem. Technol.*, **56**, 1101 (2022), <https://doi.org/10.35812/CelluloseChemTechnol.2022.56.98>
- <sup>22</sup> L. H. Li, J. C. Deng, H. R. Deng, Z. L. Liu and L. Xin, *Carbohydr. Res.*, **345**, 994 (2010), <https://doi.org/10.1016/j.carres.2010.03.019>
- <sup>23</sup> A. H. Bashal, S. M. Riyadh, W. Alharbi, K. H. Alharbi, T. A. Farghaly *et al.*, *Polymers*, **14**, 386 (2022), <https://doi.org/10.3390/polym14030386>
- <sup>24</sup> Y. Li, Y. Zhou, Z. Wang, R. Cai, T. Yue *et al.*, *Foods*, **10**, 3135 (2021), <https://doi.org/10.3390/foods10123135>
- <sup>25</sup> V. G. L. Souza, M. M. Alves, C. F. Santos, I. A. C. Ribeiro, C. Rodrigues *et al.*, *Coatings*, **11**, 646 (2021), <https://doi.org/10.3390/coatings11060646>
- <sup>26</sup> S. K. Baek and K. B. Song, *LWT*, **89**, 269 (2018), <https://doi.org/10.1016/j.lwt.2017.10.064>
- <sup>27</sup> L. C. Almeida, S. G. Segura, N. Bocchi and E. Brillas, *Appl. Catal. B: Environ.*, **103**, 21 (2011), <https://doi.org/10.1016/j.apcatb.2011.01.003>